

Time Frequency-Domain Memory for Heat Demand Prediction in Intelligent Energy Networks

Yang Xu¹, Jiyang Xie¹, Zhanyu Ma^{1*}, Hailong Li²

1 Pattern Recognition and Intelligent Systems Lab., Beijing University of Posts and Telecommunications, Beijing 100876, China

2 School of Business, Society & Engineering, Mälardalen University, Vasteras, Sweden

(*: Corresponding Author)

ABSTRACT

Heat demand prediction is a notable research topic in intelligent energy networks (IENs), due to the rapid growth of heat demand in cities. Given that hourly heat demand data can be considered as a time series data recording and well analyzed by time series seasonal decomposition algorithms, we develop a variant of the recurrent neural network (RNN), namely time frequency-domain memory (TFDM). The TFDM combines fast Fourier transform (FFT) and long short-term memory (LSTM) model to preserve memory of the series in both time and frequency domains, and cascades a residual block to introduce the impact factors (*e.g.*, weathers). In the experiments, we compare the proposed TFDM with various referred methods on a heat demand dataset. The experimental results show that the proposed TFDM has significant performance improvement in the heat demand prediction.

Keywords: Intelligent energy networks (IENs), heat demand prediction, time series prediction, time-frequency domain analysis, long short-term memory (LSTM)

1. INTRODUCTION

Intelligent Energy Networks (IENs) are intelligently optimized energy exchange networks including smart grids, smart district heating (DH) networks, and smart natural gas (NG) networks that share information between energy producers and consumers, and provide decision supports for the producers [1]. In recent years, due to the rapid growth of energy demand, especially

heat demand, the IENs have grown moderately and require high-precision prediction algorithms for the energy demand [2, 3]. Same in the district heating networks, it is important to adjust heat supply dynamically to response the heat demand and reduce the peak value of the heat supply in order to improve the efficiency of the heat supply and save costs [4, 5].

Researchers around the world focus on performance improvement of heat demand prediction and have conducted extensive researches on heat demand prediction. Numerous methods and their variants have been proposed for the goal. Cui *et al.* [6] proposed an improved autoregressive integrated moving average with exogenous (ARIMAX) to deal with the mutation data structures caused by external factors in the field of energy demand prediction. A multi-variable prediction method was introduced for heat demand prediction based on support vector regression (SVR) to improve precision of the prediction [7]. Meanwhile, the authors in [8] implemented the SVR with Firefly searching algorithm to predict heat demand for different prediction horizons. References [9] and [10] developed Gaussian mixture models (GMMs) to analyze impacts of various factors on heat demand and conducted heat demand predictions by the GMMs. In addition to the aforementioned conventional machine learning methods, artificial neural network (ANN) models have been used to predict heat demand, including feedforward neural networks (FFNN) [11], Elman neural networks (ENN) [12], nonlinear autoregressive (NARX) neural networks [13, 14].

While predicting heat demand, effective heat demand series decomposition is vital for the precision of

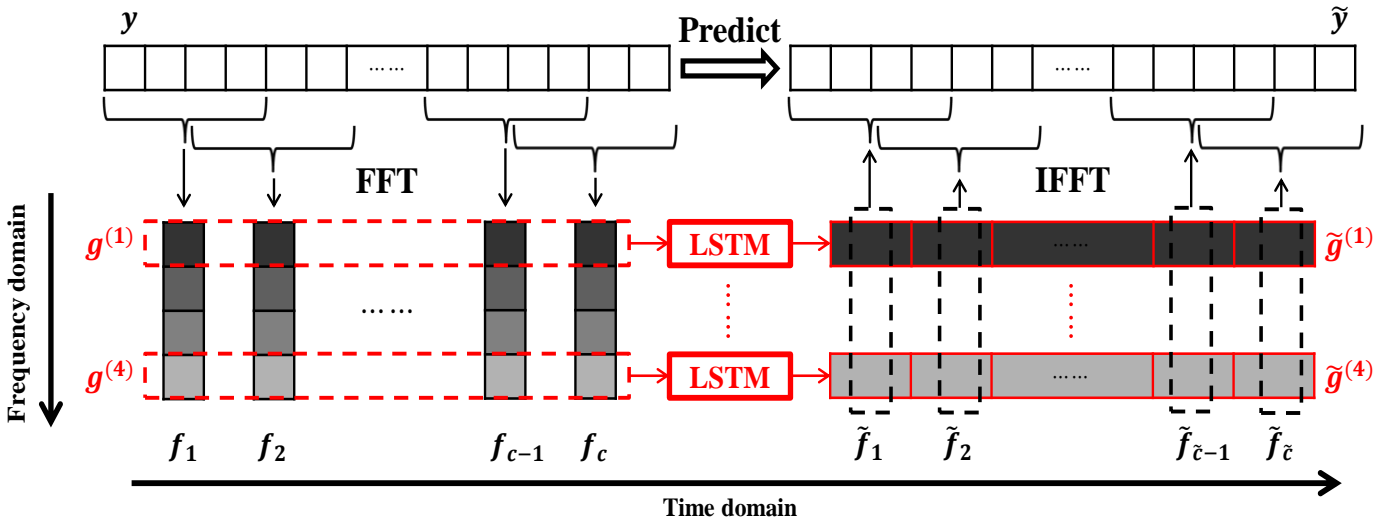


Fig 1 Model structure of the time frequency-domain memory (TFDM) without the residual block (assuming $m = 4$).

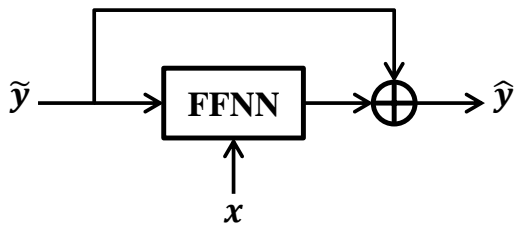


Fig 2 The structure of the residual block.

its prediction. Xie *et al.* [15] built a variant of the ENN called SEA (STL-ENN-ARIMA) model, which is a hybrid neural network, to improve the heat demand prediction performance by time series seasonal decomposition. In [15], they utilized the seasonal-trend decomposition algorithm (STL in short) [16] to decompose the heat demand series into seasonal and trend components, following ENNs and an ARIMA to predict the components, respectively. In the end, their predictions were combined together as the final heat demand predictions. Although the seasonal decomposition can only decompose the series into few frequency components, it presents strong effectiveness on heat demand prediction.

In this paper, we propose a generalization of the SEA model named time frequency-domain memory (TFDM), which extends the seasonal decomposition to the fast Fourier transform (FFT). Theoretically, the TFDM decomposes a series into equal-interval frequency bands rather than setting periods by hand. After integrating all the FFT outputs as a spectrogram, we apply long short-term memory (LSTM) models to preserve memory of the series in both time and frequency domains and predict the trend of each frequency component in the red

dashed squares in Figure 1, obtaining intermediate predictions and re-transform them by the inverse fast Fourier transform (IFFT). In addition, to introduce impactful factors including ambient temperature, direct solar irradiance, and wind speed for prediction performance improvement, we cascade a residual block.

2. MODEL DESCRIPTION

2.1 Time Frequency-Domain Memory (TFDM)

In this section, we introduce frequency information of the heat demand data series into the heat demand prediction model. Figure 1 shows the model structure of the time frequency-domain memory (TFDM).

It is known that the Fourier transform (FT), a well-known time-frequency transform, can decompose a signal in time domain into its constituent frequencies [17]. Since the continuous heat demand measurement can be sampled into a discrete time series, we can introduce the discrete Fourier transform (DFT) to process the heat demand series. Here, we actually apply the fast Fourier transform (FFT) [18], a fast algorithm of the DFT, in the model to reduce time we cost.

We firstly divide the n -length original heat demand data series y into several m -length frames where m , a power of 2, is the sliding window size. Note that we set the sliding step of the sliding window as $m/2$ and we can obtain $c = (2n - m)/m$ frames assuming that $2n$ can be divided by m with no remainder.

After transforming each m -length original heat demand data frames into the frequency domain with the m -point FFT, we can obtain c frequency frames $\{f_1, \dots, f_c\}$ of which each element represents the

Table 1 Comparisons of MAPE for the proposed TFDM with different m , hidden layer numbers l , and node numbers p . Note that the best and the second best results are marked in **bold** font and underline, respectively.

l	4			8		
	5	15	20	5	15	20
4	11.15%±0.12%	9.50%±0.13%	8.56%±0.08%	11.18%±0.06%	8.08%±0.17%	6.47%±0.14%
8	11.75%±0.09%	10.32%±0.11%	9.50%±0.10%	11.59%±0.09%	8.90%±0.20%	7.33%±0.16%
16	12.01%±0.11%	10.37%±0.09%	9.52%±0.10%	11.94%±0.19%	8.86%±0.11%	7.31%±0.14%
32	5.54%±0.04%	4.99%±0.03%	4.76%±0.05%	5.52%±0.02%	4.71%±0.08%	<u>4.75%±0.08%</u>

Table 2 Comparisons of RMSE for the proposed TFDM with different m , hidden layer numbers l , and node numbers p . Note that the best and the second best results are marked in **bold** font and underline, respectively.

l	4			8		
	5	15	20	5	15	20
4	24.33±0.23	19.11±0.17	16.33±0.16	24.45±0.39	15.11±0.33	10.92±0.19
8	25.33±0.19	20.42±0.17	18.11±0.25	24.86±0.36	16.87±0.18	12.72±0.17
16	25.44±0.15	20.22±0.14	17.82±0.19	25.35±0.48	16.52±0.33	12.30±0.27
32	14.17±0.13	11.53±0.07	10.67±0.00	14.18±0.15	<u>10.67±0.00</u>	10.64±0.02

Table 3 Comparisons of different methods of both MAPE and RMSE. Note that the best and the second best results are marked in **bold** font and underline, respectively.

Method	MAPE	RMSE
ARIMAX	11.87%±0.54%	44.33±1.53
SVR	8.78%±0.00%	31.91±0.00
GMM	8.80%±0.28%	32.88±0.73
FFNN	9.76%±1.09%	48.20±8.31
NARX	6.45%±0.09%	15.89±1.62
ENN	6.43%±0.04%	14.56±0.06
SEA-a1	<u>5.51%±0.02%</u>	<u>12.63±0.05</u>
SEA-b1	6.43%±0.04%	15.56±0.03
TFDM	4.71%±0.08%	10.67±0.00

frequency respond. Then, the i^{th} elements of the c frames can be combined into a time series $g^{(i)} = [f_1^{(i)}, \dots, f_c^{(i)}], i = 1, \dots, m$ for the corresponding frequency, which can illustrate the trend of the frequency in time domain.

In the next step, $g^{(1)}, \dots, g^{(m)}$ are utilized to train m different long short-term memory (LSTM) [19] models, predicting \tilde{c} steps by the LSTM models and obtaining m predicted frequency response series which are named as $\tilde{g}^{(1)}, \dots, \tilde{g}^{(m)}$. Then, $\tilde{f}_j = [\tilde{g}_j^{(1)}, \dots, \tilde{g}_j^{(m)}], j = 1, \dots, c$ are integrated by $\tilde{g}^{(1)}, \dots, \tilde{g}^{(m)}$, following the inverse fast Fourier transform (IFFT) outputting the heat demand prediction series \tilde{y} as shown in Figure 1. The overlapped parts in $\tilde{f}_1, \dots, \tilde{f}_{\tilde{c}}$ will be integrated by averaging.

However, one shortage of the aforementioned structure is that it cannot introduce impactful factors to improve prediction performance when predicting the heat demand. Thus, we cascade a residual block after it as shown in Figure 2. The residual block uses a feedforward neural network (FFNN) as the base model to combine the aforementioned heat demand prediction \tilde{y} and the impactful factors x . The residual values between \tilde{y} and the actual values y can be estimated and added into \tilde{y} to obtain more precise heat demand prediction \hat{y} .

2.2 Performance Evaluation

To evaluate the performance of the proposed heat demand prediction models and the referred methods, we introduce mean absolute percentage error (MAPE) and root mean squared error (RMSE), which are commonly used evaluation metrics in the regression tasks, to measure the relative and absolute errors of the predictions in the test set, respectively. Here, the MAPE can be defined as

$$\text{MAPE} = \frac{1}{n} \sum_{i=1}^n \frac{|y_i - \hat{y}_i|}{y_i} \times 100\%, \quad (1)$$

here y_i and \hat{y}_i are the i^{th} -hour actual heat demand value and the corresponding prediction value, and n is data point number in the test set. In addition, the RMSE can be defined as

$$\text{RMSE} = \sqrt{\frac{1}{n} \sum_{i=1}^n (y_i - \hat{y}_i)^2}. \quad (2)$$

3. EXPERIMENTAL RESULTS AND DISCUSSIONS

3.1 Data Description

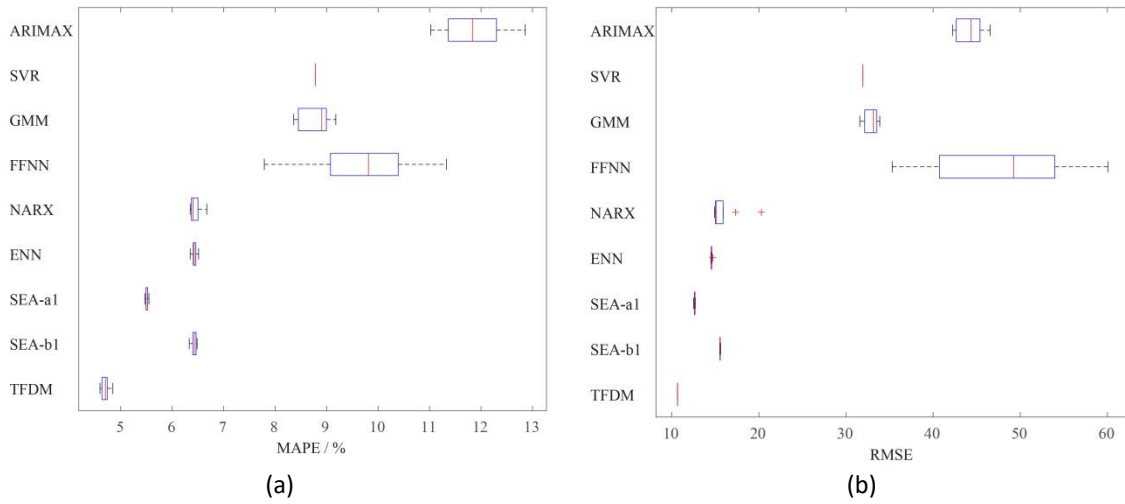


Fig 3 Boxplots of (a) MAPE and (b) RMSE.

Table 4 P -values of MAPE and RMSE between the proposed TFDM and the referred methods. Note that $p \leq 0.05$ indicates significance level of the Student's t -test.

	ARIMAX	SVR	GMM	FFNN	NARX	ENN	SEA-a1	SEA-b1
MAPE	6.72E-19	4.66E-30	1.46E-19	4.45E-11	1.10E-19	3.07E-22	4.47E-17	4.21E-22
RMSE	6.15E-23	1.02E-64	1.92E-25	7.03E-11	1.52E-08	1.46E-31	1.91E-27	1.95E-38

In this paper, we conducted experimental analysis using the hourly measured data during the period of 2008-2011 which includes the heat demand and impactful factors (*i.e.*, the ambient temperature, the direct solar irradiance, and the wind speed). The dataset was divided into a training set containing data from 2008 to 2010 (26,304 hours) and a test set containing the others (8,760 hours). We conducted the normalization as data preprocessing, following the models training. Here, we normalized all the training heat demand data and impactful factors by their respective means and standard deviations, same as the method in [15].

3.2 Heat Demand Prediction

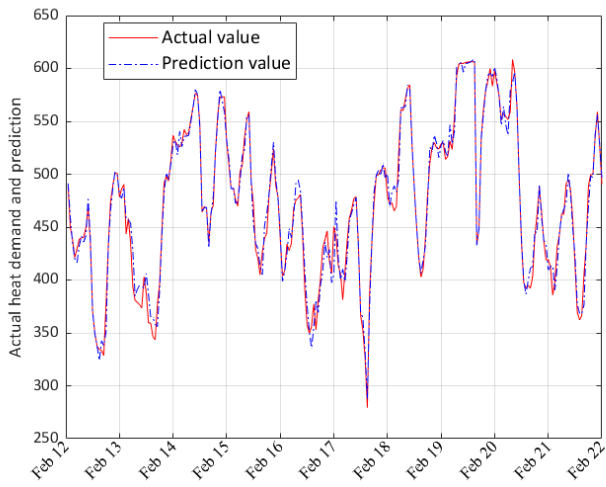
Firstly, heat demand predictions were conducted to investigate the best selection of hyperparameters, *i.e.*, point number m of the FFT, and hidden layer number l and node number p of the FFNN in the residual block. Here, we selected m from $\{4,8,16,32\}$, l from $\{4,8\}$, and p from $\{5,15,20\}$ for the comparisons and each model with different group of the hyperparameters is trained for 10 times with random initial settings to obtain the means and standard deviations of the MAPE and the RMSE. Table 1 and Table 2 show the experimental results.

From the tables, the models with $m = 32$ significantly outperform the others, while those with $m = 4,8,16$ have similar performance in the same FFNN

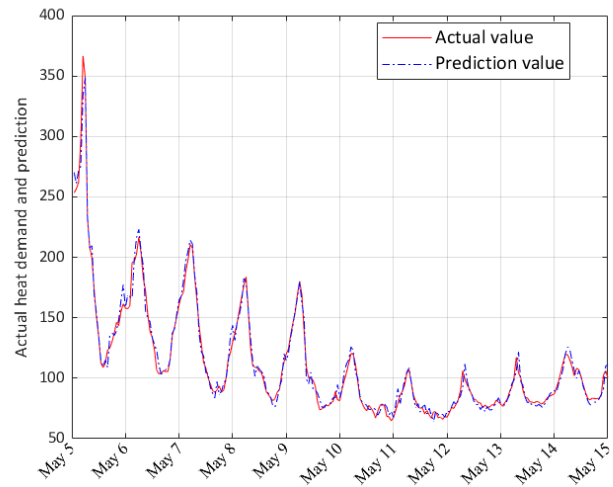
structures. Meanwhile, the model with $m = 32, l = 8, p = 15$ achieves the best among the other models on MAPE and that with $m = 32, l = 8, p = 20$ achieves the best on RMSE. Actually, they obtain comparable performance with each other, while the former has fewer parameters. Therefore, we select the model with $m = 32, l = 8, p = 15$ as the best model structure.

We then evaluated the performance of the proposed TFDM with various referred methods including conventional machine learning methods (autoregressive integrated moving average with exogenous (ARIMAX) [6], support vector regression (SVR) [20], and Gaussian mixture model (GMM) [9]) and deep neural networks (FFNN [11], ENN [12], NARX [13, 14], and SEA [15]), versions of the SEA model, named as SEA-a1 and SEA-b1, are compared. All the models are trained for 10 times with random initial settings as well. The experimental settings of the referred methods were according to [15].

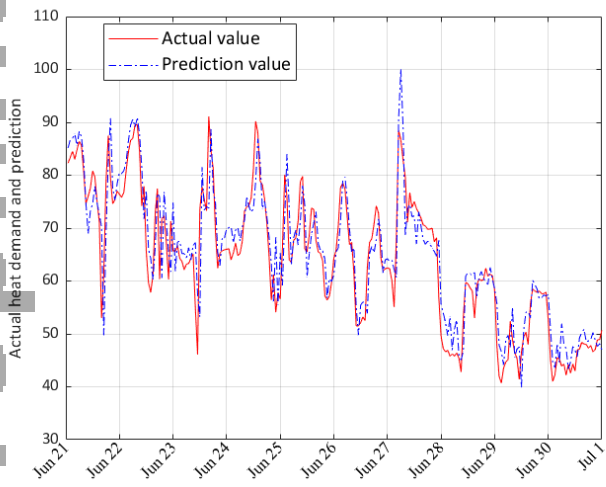
Table 3 shows the comparisons of MAPE and RMSE in the test set. The proposed TFDM outperforms all the referred methods over 0.80% on MAPE and 2.00 on RMSE. Meanwhile, boxplots are illustrated in Figure 3, which present that the proposed TFDM achieves the best performance on both the MAPE and the RMSE. The boxplots of the proposed TFDM on both the MAPE and the RMSE respectively are more compact than most of the other methods, which mean that the proposed TFDM has more steady performance.



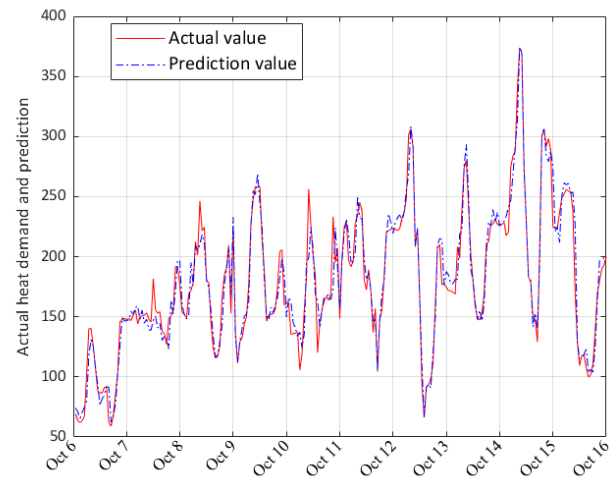
(a) February 12th – 21st.



(b) May 5th - 14th.



(c) June 21st – 31st.



(d) October 6th – 15th.

Fig.4 Comparisons between actual heat demand values (in MW) and prediction values (in MW) in four randomly selected date intervals. The date annotations in the x-axis mean the start of the day.

In addition, The Student's t -test is also conducted between the evaluation metrics of the proposed TFDM and those of the referred methods, respectively, where the statistical significance level is set as 0.05 ($\alpha = 0.05$). As shown in Table 4, given that all the p -values are smaller than 0.05 even 1×10^{-10} , the MAPE and the RMSE of the proposed TFDM are significantly different with those of the referred methods which means that the proposed TFDM has significant performance improvement.

Figure 4 illustrates four groups of comparisons between the actual heat demand values (in million Watt, MW) and the prediction values (in MW) obtained by the proposed TFDM in randomly selected date intervals. According to Figure 4, the predicted curves are close enough to their corresponding actual heat demand curves and can greatly reflect the changes of the actual

ones. This means that the proposed TFDM performs well in the heat demand prediction task.

3.3 Discussions

In this section, we discuss the reasons why the proposed TFDM is more effective than the referred methods. Firstly, similar with the principles of the SEA model [15] and seasonal decomposition, the proposed TFDM decomposes the original heat demand series into several seasonal components with distinct frequencies, which would lead the proposed TFDM to further understanding of the whole series in frequency domain and modeling the series powerfully. Moreover, an m -point FFT which can be considered as a time-frequency memory integrates information in an m -length window. This helps the model "seeing further" than a

conventional RNN when m is large, which is an additional ability of the FFT.

4. CONCLUSIONS

In this paper, we proposed a heat demand prediction method, namely the time frequency-domain memory (TFDM), based on the fast Fourier transform (FFT) and the long short-term memory (LSTM) models. Given that the model cannot introduce impactful factors, including the ambient temperature, the direct solar irradiance, and the wind speed, we cascaded a residual block to take these factors into consideration. In the experiments, we compared the proposed TFDM with various referred methods on the heat demand dataset and experimental results show that the proposed TFDM has significant performance improvement. Future work will focus on the approaches combining the impact factors into the model illustrated in Figure 1, rather than adding a residual block.

ACKNOWLEDGEMENT

This work was supported in part by the National Key R&D Program of China under Grant 2019YFF0303300 and under subject II No. 2019YFF0303302, in part by National Natural Science Foundation of China (NFSC) No. 61773071, 61922015, and U19B2036, in part by the Beijing Academy of Artificial Intelligence (BAAI) under Grant BAAI2020ZJ0204, and in part by the Beijing Nova Programme Interdisciplinary Cooperation Project under Grant Z191100001119140.

REFERENCE

[1] Ma Z, Xie J, Li H, et al. The role of data analysis in the development of intelligent energy networks. *IEEE Network* 2017; 31(5): 88-95.

[2] Sun Q, Li H, Ma Z, et al. A comprehensive review of smart energy meters in intelligent energy networks. *IEEE Internet of Things Journal* 2016; 3(4): 464-479.

[3] Liu L, Zhao Y, Chang D, et al. Prediction of short-term PV power output and uncertainty analysis. *Applied Energy* 2018; 228: 700-711.

[4] Hu J, Vasilakos A. Energy big data analytics and security: challenges and opportunities. *IEEE Transactions on Smart Grid* 2016; 7(5): 2423-2436.

[5] Eseye A T, Lehtonen M, Tukiä T, et al. Day-ahead Prediction of Building District Heat Demand for Smart Energy Management and Automation in Decentralized Energy Systems. *IEEE 17th International Conference on Industrial Informatics (INDIN)* 2019.

[6] Cui H, Peng X. Short-term city electric load forecasting with considering temperature effects: an improved

ARIMAX model. *Mathematical Problems in Engineering* 2015; 1: 1-10.

[7] Zhou X, Liu QD, Liu GQ, et al. Multi-variable time series forecasting for thermal load of air-conditioning system on SVR. *Chinese Control Conference 2015*; 8276-8280.

[8] Al-Shammari E T, Keivani A, Shamshirband S, et al. Prediction of heat load in district heating systems by Support Vector Machine with Firefly searching algorithm. *Energy* 2016; 95(jan.15): 266-273.

[9] Ma Z, Li H, Sun Q, et al. Statistical analysis of energy consumption patterns on the heat demand of buildings in district heating systems. *Energy and Buildings* 2014; 85: 464-472.

[10] Ma Z, Sun Q, Li H, et al. Dynamic prediction of the heat demand for buildings in district heating systems. *International Conference on Applied Energy* 2013.

[11] Jovanović RŽ, Sretenović AA, Živković BD. Ensemble of various neural networks for prediction of heating energy consumption. *Energy and Buildings* 2015; 94: 189-199.

[12] Ma Z, Xie J, Li H, et al. Deep neural network-based impacts analysis of multimodal factors on heat demand prediction. *IEEE Transactions on Big Data* 2020; 6(3): 594-605.

[13] Ferracuti F, Fonti A, Ciabattoni L, et al. Data-driven models for short-term thermal behaviour prediction in real buildings. *Applied Energy* 2017; 204: 1375-1387.

[14] Koschwitz D, Frisch J, Van Treeck C. Data-driven heating and cooling load predictions for non-residential buildings based on support vector machine regression and NARX Recurrent Neural Network: A comparative study on district scale. *Energy* 2018; 165(PT.A): 134-142.

[15] Xie J, Guo J, Ma Z, et al. SEA: a combined model for heat demand prediction. *IEEE International Conference on Network Infrastructure and Digital Content* 2018; 71-75.

[16] Cleveland R, Cleveland W, McRae J, et al. STL: A seasonal-trend decomposition procedure based on loess. *Journal of Official Statistics* 1990; 6(1): 3-33.

[17] Bochner S, Chandrasekharan K. *Fourier transforms*. New Jersey: Princeton University Press; 1949.

[18] Cooley JW. The re-discovery of the fast Fourier transform algorithm. *Mikrochimica Acta* 1987, Vienna, Austria; 33-45.

[19] Hochreiter S, Schmidhuber J. Long short-term memory. *Neural Computation* 1997; 9(8): 1735-1780.

[20] Koutroumbas K, Theodoridis S. *Pattern Recognition*. 4th ed. Elsevier; 2008.